Computer Methods and Programs in Biomedicine 240 (2023) 107700

Contents lists available at ScienceDirect

Computer Methods and Programs in Biomedicine

journal homepage: www.elsevier.com/locate/cmpb

A Markov Model of Gap Occurrence in Continuous Glucose Monitoring Data for Realistic in Silico Clinical Trials

Martina Vettoretti*, Martina Drecogna, Simone Del Favero, Andrea Facchinetti, Giovanni Sparacino

Department of Information Engineering, University of Padova, Via G. Gradenigo 6/B, 35131 Padova, Italy

ARTICLE INFO

Article history:
Received 7 March 2023
Revised 31 May 2023
Accepted 27 June 2023

Keywords:
Continuous glucose monitoring
Data gap
Glucose sensor
Markov model
Simulation model
Sensor error

ABSTRACT

Background and objective: Continuous glucose monitoring (CGM) sensors measure interstitial glucose concentration every 1-5 min for days or weeks. New CGM-based diabetes therapies are often tested in *in silico* clinical trials (ISCTs) using diabetes simulators. Accurate models of CGM sensor inaccuracies and failures could help improve the realism of ISCTs. However, the modeling of CGM failures has not yet been fully addressed in the literature. This work aims to develop a mathematical model of CGM gaps, i.e., occasional portions of missing data generated by temporary sensor errors (e.g., excessive noise or artifacts).
Methods: Two datasets containing CGM traces collected in 167 adults and 205 children, respectively, using the Dexcom G6 sensor (Dexcom Inc., San Diego, CA) were used. Four Markov models, of increasing complexity, were designed to describe three main characteristics: number of gaps for each sensor, gap distribution in the monitoring days, and gap duration. Each model was identified on a portion of each dataset (training set). The remaining portion of each dataset (real test set) was used to evaluate model performance through a Monte Carlo simulation approach. Each model was used to generate 100 simulated test sets with the same size as the real test set. The distributions of gap characteristics on the simulated test sets were compared with those observed on the real test set, using the two-sample Kolmogorov-Smirnov test and the Jensen-Shannon divergence.
Results: A six-state Markov model, having two states to describe normal sensor operation and four states to describe gap occurrence, achieved the best results. For this model, the Kolmogorov-Smirnov test found no significant differences between the distribution of simulated and real gap characteristics. Moreover, this model obtained significantly lower Jensen-Shannon divergence values than the other models.
Conclusions: A Markov model describing CGM gaps was developed and validated on two real datasets. The model describes well the number of gaps for each sensor, the gap distribution over monitoring days, and the gap durations. Such a model can be integrated into existing diabetes simulators to realistically simulate CGM gaps in ISCTs and thus enable the development of more effective and robust diabetes management strategies.

1. Introduction

In recent decades, the therapy of type 1 diabetes (T1D) has been revolutionized by the spread of many new technologies [1],[2], such as insulin pumps [3],[4], continuous glucose monitoring sensors [5],[6], artificial pancreas systems [7–9], and decision support systems [10–11]. The use of such new technologies in diabetes therapy has been massively tested using *in silico* clinical trials (ISCTs) [12–16]. An ISCT can be defined as "the use of individualised computer simulation in the development or regulatory evaluation of a medicinal product, medical device, or medical intervention" [13]. The reason why ISCTs are so attractive is that ISCTs can be conducted at very low cost, on large populations of virtual subjects, in a short time frame and without any risk to real patients. Moreover ISCTs allow to conduct tests on a variety of settings, which often cannot be evaluated in real clinical trials, either because of limited availability of resources or because the factors to be tested are difficult to measure on real patients (e.g., carbo-

Abbreviations: T1D, type 1 diabetes; ISCT, *in silico* clinical trial; CGM, continuous glucose monitoring; SD, standard deviation.

* Corresponding author: Address: via G. Gradenigo 6/B, Padova, 35131, Italy, Telephone: +39 049 827 7595
E-mail address: martina.vettoretti@unipd.it (M. Vettoretti).

https://doi.org/10.1016/j.cmpb.2023.107700

hydrate counting error [17]). For these reasons, ISCTs are often the first testbed for new diabetes management strategies.

Performing reliable ISCTs requires the availability of a reliable simulation model. In particular, a simulation model for testing technology-based diabetes management strategies in ISCTs should include mathematical models of the patient's physiology, the technology used and the diabetes management strategy. One of the key technologies used in T1D therapy is glucose sensors; indeed, T1D patients need to monitor their glucose concentration frequently in order to precisely adjust insulin therapy and avoid dangerous hyperglycemic or hypoglycemic events. In addition to traditional fingerprick glucometers [18], minimally-invasive continuous glucose monitoring (CGM) sensors have been increasingly adopted in T1D therapy in recent years [19–21]. CGM sensors are wearable sensors that measure glucose concentration in the interstitial fluid of subcutaneous tissue almost continuously (sampling period of 1-5 minutes) and for several consecutive days or weeks [22]. The most popular CGM sensing technique is based on an amperometric electrochemical sensor placed in the subcutaneous tissue of the abdomen or arm [23].

Like any measurement system, CGM sensors are affected by measurement error, which can be evaluated by comparing CGM readings with glycemic references measured with high accuracy and precision laboratory instruments [24–26]. Several phenomena contribute to CGM sensor error, e.g., distortion introduced by blood-interstitium kinetics, imperfect sensor calibration, random measurement noise, and interfering substances [27–29]. Moreover, CGM time series can be affected by occasional transient faults [30], such as data gaps, which are portions of missing samples. Data gaps are often due to a temporary sensor error: if the sensor processing algorithm detects excessive noise or anomalies (e.g., spikes) in the signal, the corrupted part of the signal is suppressed, thus generating a gap.

Fig. 1 shows an example of a gap due to a temporary sensor error that lasts for 45 minutes, from 10:35 to 11:20.

To better simulate CGM measurements, T1D simulators, such as the University of Virginia/Padova T1D simulator and its extensions [31–33], can incorporate a mathematical model of CGM sensor error. In fact, CGM sensor error could influence the effectiveness of CGM-based diabetes management strategies. Testing CGM-based diabetes management strategies on error-free scenarios can be useful but it will likely provide optimistic results compared to more realistic simulation scenarios in which CGM sensor error is simulated [34]. In addition to simulating the inaccuracy of CGM readings, the simulation of transient CGM faults, such as data gaps, is important to allow *in silico* assessment of the robustness of CGM-based diabetes management strategies against sensor faults that commonly occur in real life. For example, a recent study suggested that data gaps can significantly affect the accuracy of glucose metrics calculated from CGM data [35], and, consequently, the performance of diabetes-management strategies relying on them.

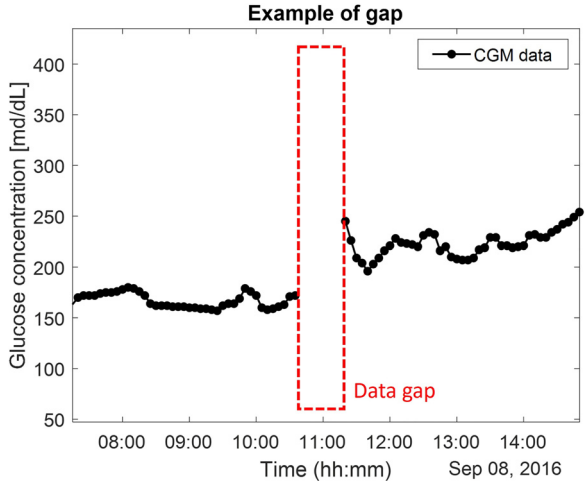

Fig. 1. A data gap in a representative real CGM sensor trace measured by the Dexcom G6 sensor in an adult subject.

While the modelling of some error components, such as the distortion introduced by blood-interstitium kinetics, calibration error and random noise, has been investigated by many literature studies [27,28,36–39], the modelling of occasional transient faults, such as data gaps, has been less investigated. A simple model to describe the occurrence of data gaps in CGM traces was proposed by Facchinetti et al. [30]; the occurrence of missing samples was modelled using a two-state Markov model, in which one state represents the status in which the sensor is functioning normally, while a second state represents the status in which the sensor shows no measurements, i.e., there is a data gap. In the same work, a second Markov model was proposed, with an additional state to allow the description of long gaps. This second model was shown to describe well the distribution of data gap durations observed in a dataset of 108 CGM traces collected by the Dexcom G4 Platinum (Dexcom, Inc., San Diego, CA) sensor on adults with T1D. However, the ability of the model to represent other important characteristics of the gaps well, for example, the frequency and timing of their occurrence, was not analyzed. In a recent study, Drecogna et al. [40] tested the model of Facchinetti et al. [30] on a dataset collected on an adult population by a new-generation CGM sensor (Dexcom G6). The study showed that the simple model of Facchinetti et al. [30] fails to describe well the characteristics of data gaps occurring in new-generation CGM sensors. Another open issue is that the model of Facchinetti et al. [30] was never tested on the pediatric population, whose different types of activities may influence the occurrence of data gaps.

The aim of the present paper is to further develop the modelling approach of Facchinetti et al. [30] to build a data gap model capable of generating gaps with the same characteristics, not only in terms of duration, but also in terms of frequency and time of occurrence, as those present in real datasets. The new model will be built on two datasets collected using a new-generation factory-calibrated CGM sensor, i.e., the Dexcom G6 sensor, on an adult population and a pediatric population, respectively.

2. Materials and methods

2.1. Datasets

The data used for this study, courtesy of Dexcom Inc. (San Diego, CA), were collected as part of a single-arm interventional clinical trial to test the effectiveness and safety of the Dexcom G6 CGM sensor. The study started on May 2016 and ended on September 2017. The inclusion criteria included: age $\geq$2 years, diagnosis of T1D or T2D on intensive insulin therapy, and willing to participate in a clinic session involving venous sampling for evaluation of study end point. The exclusion criteria included: use of acetaminophen, known allergy to medical-grade adhesives, pregnancy, and hematocrit outside the normal range. Participants were enrolled at 11 sites and located throughout the U.S.. More information on the data collection process and detailed demographic characteristics of the enrolled patients are available in the original study publications [41,42].

From data collected in the study, two datasets were extracted. The first dataset includes 203 CGM traces collected on 167 adults (18-59 years old) with T1D or T2D (36 subjects wore two sensors). The second dataset includes 285 CGM traces collected on 212 children and adolescents (6-17 years old) with T1D or T2D

(73 children/adolescents wore two sensors). In the following of this publication, the two datasets will be called “the adult dataset” and “the pediatric dataset”, respectively. In both datasets, CGM traces were collected with the Dexcom G6 sensor, which has a 10-day lifetime. In total, 133 sensors have stopped working before 10 days were elapsed since sensor insertion. Premature interruption of sensor operation is probably due to irreversible damage of the sensor from which it is not possible to recover, unlike data gaps which are generated by temporary sensor errors, after which the sensor resumes normal operation. Since modeling the premature interruption of sensor operation is out of the scope of this work, for our analysis, we selected only the traces with a minimum duration of 9 days from sensor insertion, so that we could observe the gap distribution over the entire life of the sensor. This results in two final datasets: the adult dataset, which includes 172 CGM traces, and the pediatric dataset, which includes 205 CGM traces. The two datasets were analyzed separately.

2.2. Exploratory analysis of data gaps

CGM data gaps are portions of missing data in CGM time series. In our datasets, we identified 229 and 484 data gaps in the adult and the pediatric datasets, respectively. The distribution of three main gap characteristics was analyzed: the number of gaps for each sensor, the CGM monitoring day on which the gap occurs, and the gap duration. The relative frequencies of these characteristics are shown in Fig. 2 for the adult dataset (panels (a)-(c)) and the pediatric dataset (panels (d)-(f)). It should be noted that the number of gaps per sensor was not normalized by CGM trace duration because, after excluding traces with duration of less than 9 days, the CGM traces retained in the analysis had similar duration.

Focusing on the number of gaps per sensor (Fig. 2 (a),(d)), it can be observed that about 65% of adult traces and 45% of pediatric traces have no gaps. It is also possible to observe that in the adult population most of traces with gaps have only one occurrence, whereas in the pediatric population CGM traces with two or more gaps are more common. Therefore, the incidence of data gaps is higher in the pediatric population than in the adult population.

Panels (b) and (e) in Fig. 2 show that the occurrence of data gaps varies with the time from sensor insertion and, in particular, more gaps occur at the end of sensor life in both populations. A higher frequency of data gaps is also observed for the day of sensor insertion, where sensor performance is less stable.

In panels (c) and (f) of Fig. 2, the distributions of data gap durations are shown in logarithmic scale to facilitate visualization of the histogram tails. The peak of the distributions is at 25 minutes in the adult population and at 30 minutes in the pediatric one. After the peak, the frequency of gaps decreases as the gap duration increases, with a maximum duration observed around 95 minutes, in the adult population, and 120 minutes in the pediatric population. Quite different trends are present for gap durations shorter than the peak duration: in adults, the distribution before the peak is fairly uniform, while in children the relative frequency of gaps is increasing for durations between 10 and 30 minutes.

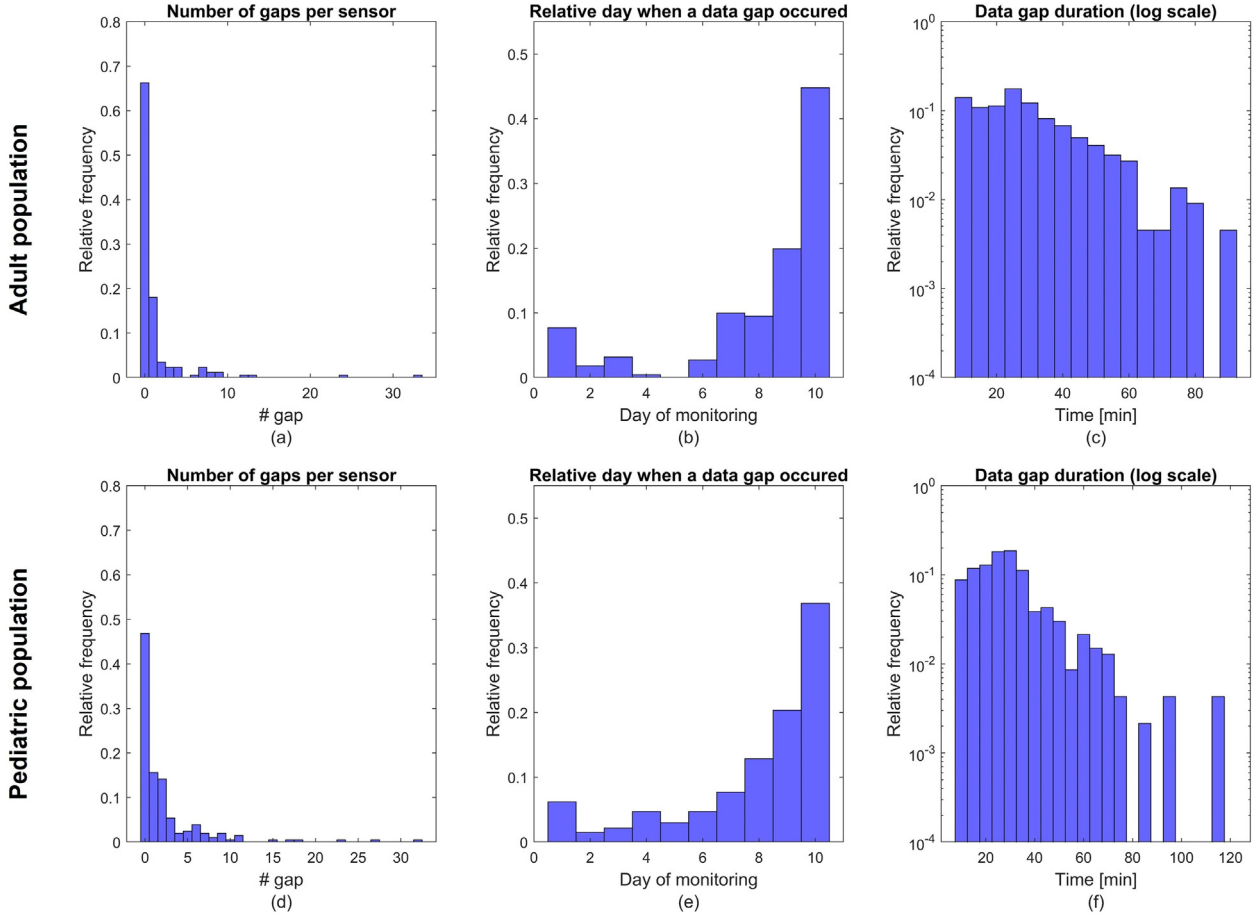

Fig. 2. Data gap characteristics: number of gaps for each sensor (left), gap distribution over monitoring days (middle), data gap duration (right). The upper panels (a), (b), and (c) refer to the adult population, while the lower panels (d), (e), and (f) refer to the pediatric population.

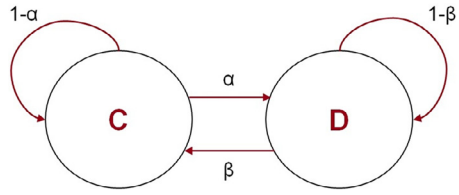

Fig. 3. Two-state Markov model: in state C the sensor is working regularly, in state D the sensor measurement is missing due to a data gap.

2.3. Design of four candidate data gap models and estimation of their parameters

Four Markov models were designed to describe the occurrence and the duration of data gaps observed on the available datasets, as shown in Fig. 2. The candidate models include the model previously proposed by Facchinetti et al. [30] (Model 1). In the following subsections, we present each candidate model and the estimators of its parameters.

2.3.1. Model 1: Two-state Markov model

The first model is a two-state Markov model (Fig. 3), first proposed by Facchinetti et al. [30].

This simple model has two states: in state C ("connected") glycemic measurements are collected regularly by the sensor, while in state D ("disconnected") the data are missing, i.e., a gap occurs. Transitions between states are governed by four probability values. If the sensor is functioning normally (state C), α is the probability that the next sample will be missed (transition from C to D), while $(1-\alpha)$ is the probability that the sensor will continue to function regularly (transition from C to C). If the current sample is missing (state D), β is the probability that the next sample is also missing, whereas the probability that the system will resume normal operation is $(1-\beta)$. Calling d the duration of a gap, the probability that a gap lasts for k samples, according to this model, is:

$$P[d=k] = \beta^{k-1} \cdot (1-\beta) \tag{1}$$

that corresponds to k−1 consecutive D-D transitions followed by a sensor reconnection (transition from D to C). The transition probabilities α and β can be estimated as:

$$\hat{\alpha} = \frac{\#\ of\ data\ gaps}{\#\ of\ regular\ samples} \tag{2}$$

$$\hat{\beta} = \frac{\#\ of\ missing\ samples\ preceded\ by\ a\ missing\ sample}{\#\ of\ missing\ samples} \tag{3}$$

where the regular samples are those that are not missing.

This first model is very simple; it is based on the hypothesis that both α and β are constant over time: this means that in this case the probability of having a gap and the probability of their duration do not change over time. Since these assumptions do not reflect the actual trend of observed gaps on real data (Fig. 2), in the models proposed below we will abandon them, for example by making α time-dependent (Model 2) or by adding other states and parameters to the model (Model 3, Model 4).

2.3.2. Model 2: Two-state Markov model with time-dependent probability of gap

Model 2 has the same structure as the first one (Fig. 3) with the only difference being that in Model 2 α is made time-dependent to better describe the distribution of the gaps across the monitoring days.

In particular, assuming that the probability of having a gap may vary for each monitoring day, α is defined as a staircase function of time from sensor insertion, t, in which each step has a one-day duration. The values of α for each day of CGM monitoring can then be estimated as in Eq. (4), whereas the estimation of the β probability remains the same as in Model 1:

$$\hat{\alpha}(t) = \alpha_k\ in\ day\ k\ from\ sensor\ insertion$$
$$\hat{\alpha}_k = \frac{\#\ of\ data\ gaps\ in\ day\ k}{\#\ of\ regular\ samples\ in\ day\ k} \tag{4}$$

$$\hat{\beta} = \frac{\#\ of\ missing\ samples\ preceded\ by\ a\ missed\ sample}{\#\ of\ missing\ samples} \tag{5}$$

It should be noted that, with the definition provided in Eq. (4), $\hat{\alpha}(t)$ is defined by 10 different parameters $\hat{\alpha}_k$, k=1, ..., 10. Alternatively, to minimize the number of parameters to be estimated, we can group days with similar gap probabilities together and then estimate a different α value for each group of days with similar gap probability. Of course, this is an operator-dependent decision that can be modified according to preference and need. More details on the reduction of the α(t) parameters for the two populations considered in this paper can be found in the Supplementary Material (section S1).

2.3.3. Model 3: (n+1)-state Markov model with time-dependent probability of gap

Model 3 aims to improve the description of the gap duration by adding new states. The resulting model, shown in Fig. 4, is similar to the second model proposed by Facchinetti et al. [30], except that in this case the parameter α is time-dependent. Model 3 includes a state C to describe the normal operation of the sensor and n states D_1, D_2, ..., D_n to describe sensor gaps that last for 1, 2, ..., n samples.

While the α(t) estimator is the same as in Model 2 (Eq. (4)), β is no longer constant for the entire duration of the gap, but it changes for each additional missing sample. In particular, the parameter β_1 describes the probability that the sensor gap will last more than one sample, given that a gap has just begun. The parameter β_2 represents the probability that the gap will last more than 2 samples, given that two samples are already missing. In general, the β_n parameter describes the probability of having a gap of duration >n samples, given a sequence of n consecutive missing samples. The estimators for the β_1, β_2, ..., β_n parameters of Model

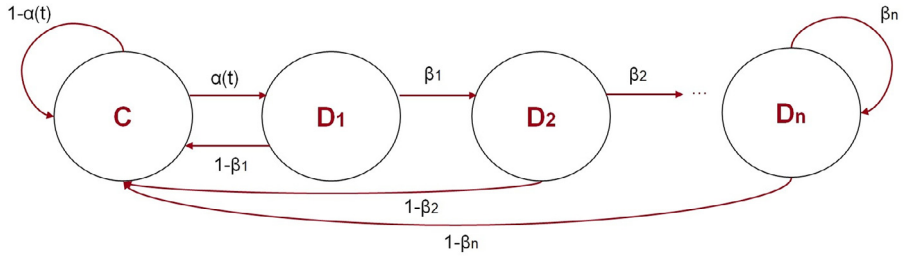

Fig. 4. The structure of Model 3: one state C describes the normal operation of the sensor, n states D_1,D_2, ..., D_n describe the occurrence of gaps.

3 are the following:

$$\hat{\beta}_1 = \frac{\#\ of\ data\ gap\ lasting\ at\ least\ two\ samples}{\#\ of\ data\ gap\ lasting\ at\ least\ one\ samples}$$
$$\hat{\beta}_2 = \frac{\#\ of\ data\ gap\ lasting\ at\ least\ three\ samples}{\#\ of\ data\ gap\ lasting\ at\ least\ two\ samples} \quad (6)$$
$$\ldots$$
$$\hat{\beta}_n = \frac{\#\ of\ data\ gap\ lasting\ at\ least\ (n+1)\ samples}{\#\ of\ data\ gap\ lasting\ at\ least\ n\ samples}$$

A key point in building the model concerns the choice of the number of states and parameters used to describe the sensor gap; the objective is to achieve a good description of the data gap duration distribution, while maintaining small the number of states and β parameters. In Fig. 2 panels (c) and (f), it can be observed that the distribution of gap duration changes its trend around a duration value of 25 minutes. In order to capture this trend change, and considering the memoryless property of Markov models, four states are needed to describe the occurrence of gaps, i.e., D_1, D_2, D_3, D_4. Therefore, the final structure of Model 3 is the one of Fig. 4 with n=4, with parameters α(t), β_1, β_2, β_3, β_4.

Note that the four β parameters need not be different from each other. To limit the model complexity, some β parameters can be fixed to the same values without relevantly deteriorating the model goodness of fit. In this work, for the adult population only, we decided to reduce the β parameters from four to two probability values: $\beta_{1,red}$ which is the probability that a gap lasts 1,2, or 3 samples and $\beta_{4,red}$ which is the probability of having a gap of 4 or more samples. More details on parameter reduction can be found in the Supplementary Material (section S2).

2.3.4. Model 4: (n+2)-state Markov model with time-dependent parameters

Models 1-3 assume that the gaps are equally distributed among the sensors. However, as can be seen in the left panels of Fig. 2, most CGM traces contain no gaps, and some CGM traces contain one or more gaps. To describe well the distribution of the number of gaps per sensor, Model 4 is proposed, the structure of which is shown in Fig. 5. This model includes (n+2) states, of which n are used to describe the gap occurrence, as in Model 3, and the other two describe the normal operation of the sensor. In particular, C_1 corresponds to the normal operation of the sensor that has never had a gap up to that time; C_2 describes the normal functioning of a sensor that has already experienced at least one gap. The transition from C_1 to D_1 is governed by α_1(t), which represents the probability of having a gap for a sensor that has never had a gap before. Instead, α_2(t) is the transition probability between state C_2 and D_1, which represents the chance that a sensor that has already had a gap will have another gap. The estimation of the β parameters is the same as in Model 3 (Eq. (6)), while α_1(t) and α_2(t) are both defined as a staircase function of time from sensor insertion t:

$$\hat{\alpha}_1(t) = \alpha_{1k}\ in\ day\ k\ from\ sensor\ insertion$$
$$\hat{\alpha}_{1k} = \frac{\#\ of\ first\ data\ gaps\ in\ day\ k}{\#\ of\ regular\ samples\ until\ the\ first\ gap\ in\ day\ k} \quad (9)$$
$$\hat{\alpha}_2(t) = \alpha_{2k}\ in\ day\ k\ from\ sensor\ insertion$$
$$\hat{\alpha}_{2k} = \frac{\#\ of\ data\ gaps\ after\ the\ first\ one\ in\ day\ k}{\#\ of\ regular\ samples\ after\ the\ first\ gap\ in\ day\ k} \quad (10)$$

Since we decided to set n=4 for our specific case study, the implementation of Model 4 considered in this work has 6 states in total, namely C_1, C_2, D_1, D_2, D_3, D_4. As for the other models, one can decide to use different values of α_1 and α_2 for each day of monitoring k (obtaining 10+10 different parameters), or one can group days with similar gap probabilities, and then consider a different α_1 or α_2 value for each group of days with similar gap probability. Again, this is an operator-dependent decision that can be modified according to preferences and needs. In this work, we decided to group some of the days in order to limit the model parameters to be estimated. The details on the groupings adopted for the two populations are given in the Supplementary Material (section S3).

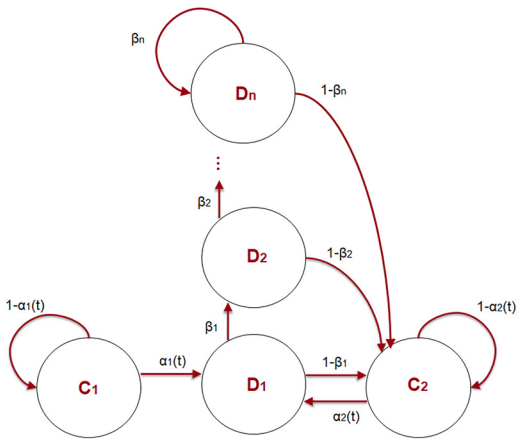

Fig. 5. The structure of Model 4: two states C_1 and C_2 describe the normal operation of the sensor, n states D_1, D_2, ..., D_n describe the gap occurrence.

2.4. Assessment of the four candidate models

The evaluation of the four candidate models is based on the comparison of the characteristics of the gaps simulated by the models with those of the gaps observed on the real datasets. In particular, we first identified the models on the entire datasets and we assessed their goodness of fit on the same data using a Monte Carlo simulation approach. Then, to evaluate the generalization ability of the models, we divided the data into a training set and a test set, we identified the models on the training set and we tested them on the test set from both qualitative and quantitative perspectives. Details of the approaches used for model assessment are described in the following subsections.

2.4.1. Assessment of model goodness of fit on the entire population

First, we assessed the model goodness of fit on the entire datasets, considering the adult and the pediatric population separately. The four candidate models were identified using all available adult/pediatric data. Then, the performances of each model were evaluated on the entire datasets using a Monte Carlo simulation approach, based on the following steps.

- Step 1: Generation of N = 100 simulated datasets, of the same size of the real one, in which data gaps are simulated with the identified model.
- Step 2: For each simulated dataset, computation of the relative frequencies of the three gap characteristics shown in Fig. 2, i.e., the number of gaps per sensor, the CGM monitoring day on which the gap occurs, and the gap duration.
- Step 3: Comparison of the mean ± standard deviation (SD) of the relative frequencies obtained for the N=100 simulated datasets in the previous step and those obtained from the real dataset.

Each simulated dataset consists of M sequences of the same length as the M CGM traces of the real dataset. The samples of each simulated sequence are equal either to “0”, which represents a regular CGM sample (i.e., no gap), or to “1”, which represents a missing CGM sample (i.e., a gap). Fig. 6 shows the procedure used to simulate the sequences of a simulated dataset by using the simplest data gap model, i.e., Model 1. For each simulated trace, we

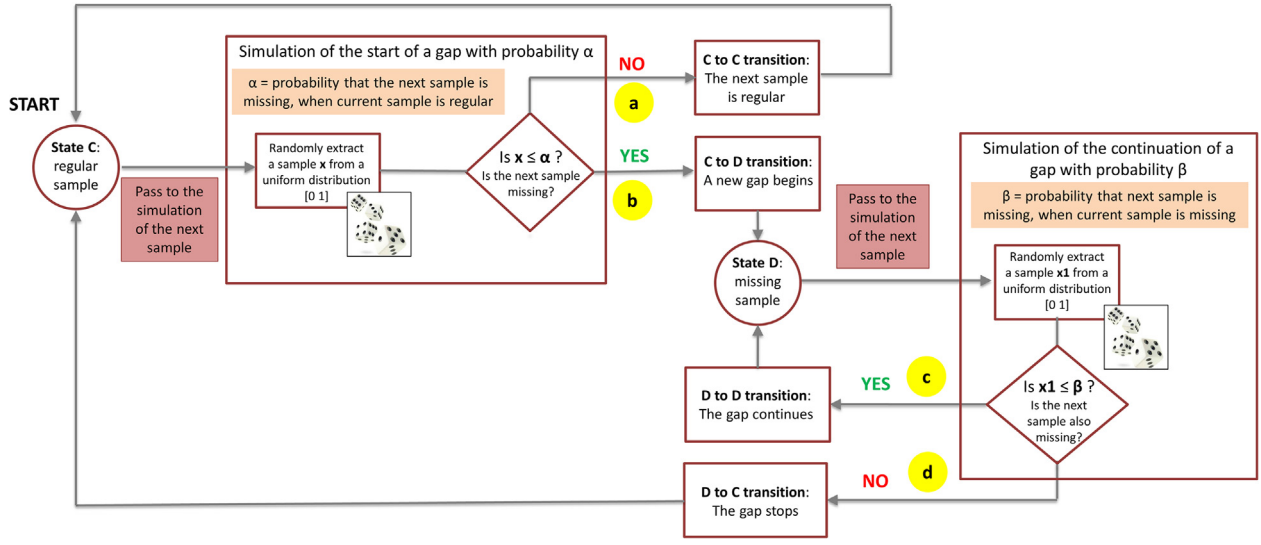

Fig. 6. Schematic representation of gap simulation for a specific CGM trace using Model 1.

start with a regular sample (state C) and then we simulate the state of the next sample (C for regular samples or D for missing samples) considering that α is the probability that the next sample is missing. To do that, we draw a sample x from a uniform distribution between 0 and 1 and compare it with the probability α that a gap begins. If x is greater than α (Fig. 6 (a)), the next sample is a regular sample (C to C transition). Then, we pass to the simulation of the following sample, extract another x value and, again, compare it with α. This mini-cycle continues until the condition $x \leq \alpha$ is satisfied (Fig. 6 (b)): in this case, the next sample is missing (C to D transition) and so the gap begins. The status of the following sample is simulated considering that β is the probability that a missing sample is followed by another missing sample. Then, to simulate whether the gap will go on or not, we draw a sample x1 from a uniform distribution between 0 and 1 and compare it with the probability β that the gap continues: if the condition $x1 \leq \beta$ is satisfied (Fig. 6 (c)), the simulated gap continues (D to D transition) and we move on to the simulation of following sample, for which we draw another x1 value and, again, we compare it with β. If the new x1 value is still $\leq \beta$, the gap continues with another missing sample. The gap simulation advances until x1 becomes greater than β (Fig. 6 (d)): in this case, the gap stops (D to C transition) and with the next sample the entire cycle starts again. This cycle is applied for each simulated trace of each simulated dataset.

In the previous paragraph, we presented the simulation approach for the simplest two-state Markov model with constant parameters, but the simulation approach is the same for more complex Markov models with time-dependent parameters: the key is to adjust the α and β values according to the model. For example, in Model 2 the α probability changes with the day since sensor insertion, so if we are simulating the k^{th} day of monitoring, we will refer to the value α_k. In Model 3 the probability β changes depending on the duration of the simulated gap: in this case, x1 will be compared with the β value specific for the current gap duration.

2.4.2. Validation of the models on the test set

To avoid the risk of overfitting the data, we also performed model validation on an independent test set not used for model parameter estimation. We randomly divided the data into a training set, containing the 70% of the CGM traces, and a test set with the other 30% of the traces. As we imposed that each subject can only be part of one of the two groups at a time, subjects with two sensors have both traces in one or the other data partition. The parameters of each of the proposed models were estimated using the training set data. The identified models were then assessed on the test set, by the Monte Carlo simulation approach described earlier. Performance on the test set was evaluated both qualitatively and quantitatively. The qualitative assessment consisted, as for the whole datasets, in comparing the mean±SD of the relative frequencies of data gap characteristics obtained for the simulated datasets with the relative frequencies of data gap characteristics of the test set. The quantitative assessment consisted of comparing the distribution of gap characteristics extracted from the simulated datasets vs. those extracted from the test set, using the two-sample Kolmogorov-Smirnov statistical test and the Jensen-Shannon divergence metric.

The two-sample Kolmogorov-Smirnov test is a non-parametric goodness-of-fit test of whether two sets of data (samples) are drawn from the same probability density function [43]. The test is based on the distance D between the empirical distribution function of the two samples. For our purpose, we applied the test to compare a data gap characteristic (e.g., the number of gaps per sensor) of a simulated dataset, with the same characteristic of the test set. The Kolmogorov-Smirnov test was applied for each of the 100 simulated datasets, with a significance level of 0.05 corrected for multiple tests according to Bonferroni: therefore, we reject the null hypothesis ("the two samples comes from the same distribution") if the p-value of each test is smaller than 0.05/m, where m is the number of considered datasets, i.e., 100, and we accept it if the p-value is greater than 0.05/m. For each gap characteristic, the p-value distribution was represented with a boxplot, and the number of simulated datasets for which the null hypothesis was accepted/rejected was counted. If a model describes the gap characteristic well, we expect that the Kolmogorov-Smirnov test will not reject the null hypothesis, i.e., that the p-values are above the adjusted significance threshold (0.0005).

Model performance was evaluated also using the Jensen-Shannon divergence [44], $JSD(P||Q)$, that is a symmetrized and smoothed version of the Kullback–Leibler divergence, $KLD(P||Q)$, which measures how different a probability density function Q is from a reference probability density function P. Specifically, the Jensen-Shannon divergence between P and Q is defined as:

$$JSD(P||Q) = \frac{1}{2}KLD(P||M) + \frac{1}{2}KLD(Q||M) \quad (13)$$

where $KLD(P||Q) = \sum P(x)log(\frac{P(x)}{Q(x)})$ and $M = \frac{1}{2}(P+Q)$.

The Jensen–Shannon divergence is 0 if the two distributions are identical, ln(2) if they are maximally different. For our purpose, we calculated the Jensen–Shannon divergence between the probability density function of gap characteristics estimated from the relative frequencies of simulated datasets and the same estimate made on the test set data. The smaller the divergence measure turns out to be, the better the model is able to reproduce the gap characteristics observed on the test set data.

3. Results

For sake of paper readability, in the following subsections we report the results obtained on the adult population only. Those obtained for the pediatric population, which would lead to a qualitatively similar discussion, are reported in the Supplementary Material (section S4).

3.1. Model fit on the entire population

The values of the model parameters estimated on the entire adult population dataset are reported in Table 1 for the four candidate models. As explained in the Supplementary Material (section S1), for Model 2 and 3 we estimated just 4 α_k values, i.e., one for days 1,7,8, one for days 2-6 and two more for days 9 and 10. Similarly, in Model 4, we estimated 3 α_{1k} values (for days 1 and 10, 2-8, and 9, respectively) and 4 α_{2k} values (for days 1-6, 7 and 8, 9, and 10, respectively).

The results of the Monte Carlo simulation on the entire adult dataset are shown in Fig. 7. In each panel, one can compare the relative frequencies of a gap characteristic on the real dataset (blue histogram) with the mean±SD values of the relative frequencies obtained for the 100 simulated datasets (red line).

Panels (a) (b) (c) in Fig. 7 show the results for Model 1. In panel (a) we can compare the real vs. simulated relative frequencies for the number of gaps for each sensor; we can observe that the model's description of the data is acceptable, but not optimal. Indeed, the model estimates that almost 30% of the traces have no gaps, while in the real dataset about 65% of the traces contain no gaps. Moreover, the number of traces with 1, 2, or 3 events is overestimated by the model. Panel (b) shows the distribution of gaps over the monitoring days. While in the real dataset the probability of having a gap in the last days since the sensor insertion is higher than in the first days, the model simulates gaps uniformly throughout the CGM monitoring period. This is due to the fact that in Model 1 α is constant over time. Panel (c) shows the distribution of gap duration using the log-scale in order to appreciate the model performance even for low probability values, which corresponds to long gap durations. The model, being characterized by a single parameter β, fails to describe the peak of the distribution at 25 min, and simulates a decreasing linear trend. The panel also shows the curve obtained from the theoretical formula that calculates the probability of having a gap that lasts for k samples using Eq. (1): since this theoretical curve (green line) and the result of the simulation (red line) are superimposable, we can confirm that the simulation algorithm works correctly and that 100 repetitions in the Monte Carlo simulation are sufficient to obtain a good estimate of the theoretical results.

The second model, Model 2, introduces a time-dependence for α. As visible in Fig. 7, the introduction of a temporal variability for α improves the description of the distribution of gaps in the monitoring days (panel (e)), whereas the description of the number of gaps per sensor (panel (d)) and the data gap duration (panel (f)) are comparable between Model 1 and Model 2.

The third model, Model 3, introduces a few more states to improve the description of the distribution of data gap durations shown in panel (i). We can observe that Model 3 describes well the observed relative frequencies of gap durations, even capturing the peak at 25 minutes. This model performs well overall, although the description of the number of gaps for each sensor (panel (g)) is still not satisfactory.

Model 4 introduces an additional state to improve the description of the relative frequencies of the number of gaps per sensor (panel (j)). This final model describes well, at least from a qualitative point of view, all the analyzed gap characteristics, with the only limitation that the number of traces with only one event is underestimated (second bin of the histogram in panel (j)).

Table 1
Estimates of α and β parameters for the four candidate data gap models identified on the adult dataset.

Models	$\hat{\alpha}$	$\hat{\beta}$
Model 1	$\hat{\alpha} = 4.65 \cdot 10^{-4}$	$\hat{\beta} = 0.7082$
Model 2	$\hat{\alpha}_{1,7,8} = 4.06 \cdot 10^{-4}$ $\hat{\alpha}_{2-6} = 7.67 \cdot 10^{-5}$ $\hat{\alpha}_{9} = 9.11 \cdot 10^{-4}$ $\hat{\alpha}_{10} = 2.20 \cdot 10^{-3}$	$\hat{\beta} = 0.7082$
Model 3	$\hat{\alpha}_{1,7,8} = 4.06 \cdot 10^{-4}$ $\hat{\alpha}_{2-6} = 7.67 \cdot 10^{-5}$ $\hat{\alpha}_{9} = 9.11 \cdot 10^{-4}$ $\hat{\alpha}_{10} = 2.20 \cdot 10^{-3}$	$\hat{\beta}_{1,red} = 0.8550$ $\hat{\beta}_{4,red} = 0.7270$
Model 4	$\hat{\alpha}_{1_{1,10}} = 4.25 \cdot 10^{-4}$ $\hat{\alpha}_{1_{2-8}} = 6.11 \cdot 10^{-5}$ $\hat{\alpha}_{1_{9}} = 1.85 \cdot 10^{-4}$ $\hat{\alpha}_{2_{1-6}} = 2.95 \cdot 10^{-4}$ $\hat{\alpha}_{2_{7,8}} = 1.80 \cdot 10^{-3}$ $\hat{\alpha}_{2_{9}} = 3.30 \cdot 10^{-3}$ $\hat{\alpha}_{2_{10}} = 6.60 \cdot 10^{-3}$	$\hat{\beta}_{1,red} = 0.8550$ $\hat{\beta}_{4,red} = 0.7270$

3.2. Validation of the models with training-test set split

To assess the generalization ability of the models and to avoid possible overfitting of the data, model parameters were identified on 70% of the total traces (121 adult traces); then, model performance was tested on the remaining 30% of traces (51 adult traces), using the Kolmogorov-Smirnov test and the Jensen-Shannon divergence.

For each gap characteristic, Fig. 8 shows the distributions of distances D (left panels) and p-values (right panels) calculated with the Kolmogorov-Smirnov test for each of the 100 simulated datasets constructed with Monte Carlo simulation. The significance level is set at 0.0005, obtained by correcting the 0.05 significance level for multiple tests m (in our case, m = 100). The performance of a model X are considered better than the one of model Y, if the distance D for model X is less than D for model Y. Moreover, a model that describes a data gap characteristic well should have a small number of simulated datasets for which the p-value is below the significance level (dashed red line). The median values of D and p-value, their 5^{th}-95^{th} percentile interval, and the percentage of p-values below the significance level are reported in Table 1 for all models.

Regarding the number of gaps for each sensor (Fig. 8, panel (a)), the distance D is almost the same for the first three models, while it decreases with Model 4. The distribution of p-values (Fig. 8, panel (b)) confirms the trend of the distances: while for the first three models almost all the p-values are below the significance level, there is a substantial improvement for Model 4 with only 12% of p-values leading to the rejection of the null hypothesis. This small percentage of p-values below the threshold is probably due to the tendency of Model 4 to underestimate the number of traces that contain only one gap.

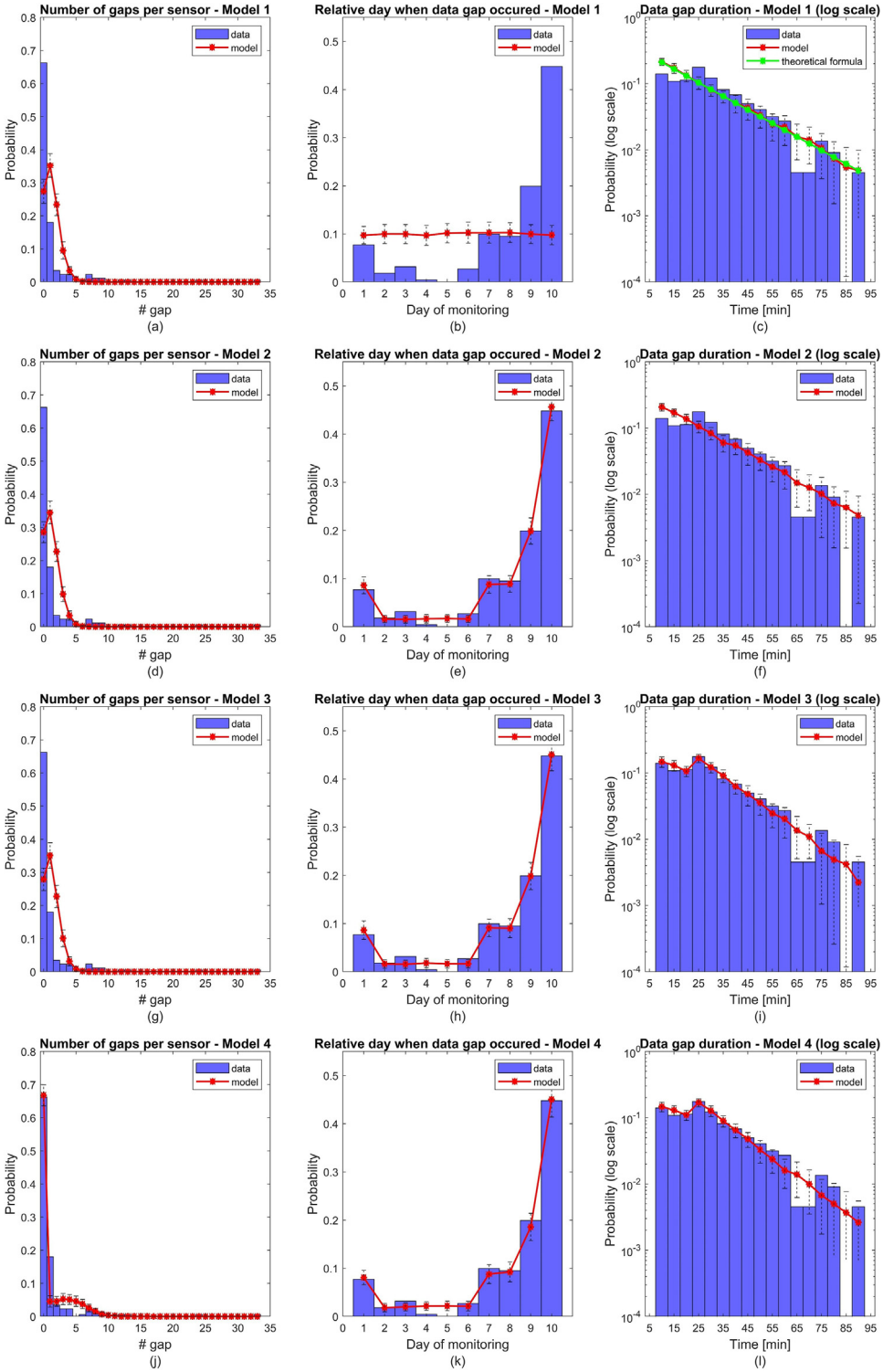

Fig. 7. Monte Carlo simulation results for all models on the adult dataset. The blue histograms represent the relative frequencies of data gap characteristics distributions. The red curves represent the mean of the relative frequencies obtained from the simulated datasets with their ±SD interval.

Concerning the distribution of the gap in the monitoring days, in Fig. 8, panels (c)(d), it can be seen that the performance improves starting from the second model, that is, from the inclusion of the time-dependence of the parameter α. From Table 2, it can be seen that with the first model all p-values are below the significance level, while for Models 2, 3, and 4 all p-values are above it.

Finally, regarding gap durations, we see from the distribution of distances D that there is an improvement in performance with Model 3 and Model 4. Regarding p-values, even for the first two models most of the p-values are above the significance level; in fact, even Model 1, the simplest one, provides a fairly satisfactory description of the distribution of gap durations, although this can be further improved with the addition of new states. This as-

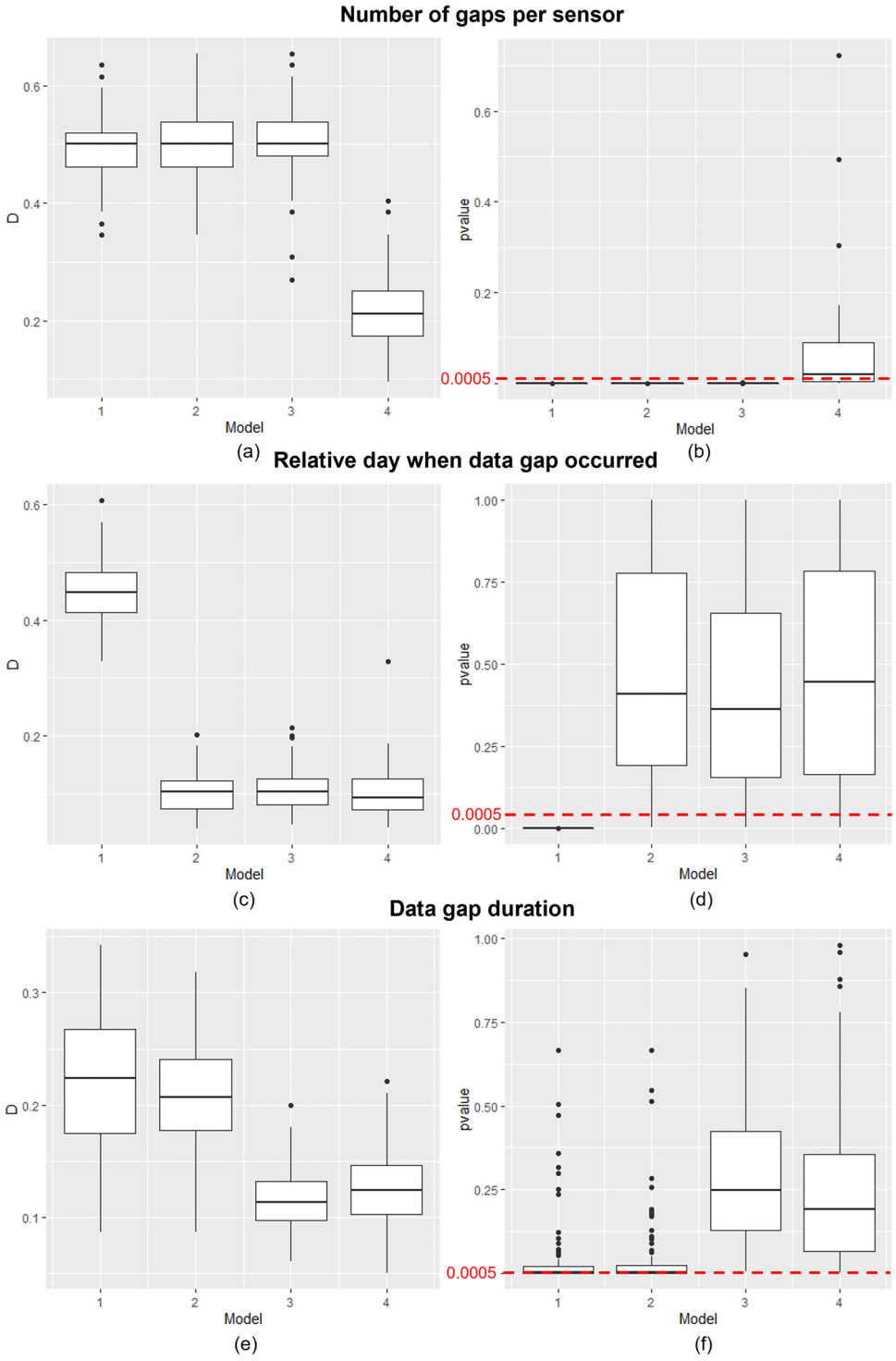

Fig. 8. Distributions of D distances and p-values calculated for each gap characteristic for each of the 100 simulated datasets with the Kolmogorov-Smirnov test (adult population).

pect is also confirmed by the p-values calculated for the last two models, which have higher values further from the significance level.

The results obtained with the Kolmogorov-Smirnov statistical test are confirmed by the Jensen-Shannon divergence whose median [5^{th} – 95^{th} percentiles] is reported in Table 3. We can see that for the number of gaps per sensor the model with lowest divergence values is Model 4; for the distribution of gap in the monitoring days Model 2, 3 and 4 get equally better results than Model 1, and for the distribution of the durations Model 3 and 4 get the best results.

In conclusion, the only model that provides a satisfactory description of all the three data gap characteristics is Model 4.

4. Discussion

A model of CGM data gaps is needed to realistically simulate CGM time series in ISCTs, thus allowing CGM-based diabetes man-

Table 2
Distances D and p-values calculated with the Kolmogorov-Smirnov test for the adult population.

		D Median [5th-95th percentile]	p-value Median [5th-95th percentile]	Num. of p-values below significance level [%]
Number of gaps per sensor	Model 1	0.50 [0.42 0.59]	1.02e-11 [2.22e-16 1.99e-08]	100
	Model 2	0.50 [0.40 0.59]	1.02e-11 [2.10e-16 1.02e-07]	100
	Model 3	0.50 [0.40 0.59]	1.02e-11 [2.20e-16 8.60e-08]	99
	Model 4	0.21 [0.11 0.32]	0.019 [2.86e-05 0.4929]	12
Relative day when data gap occurred	Model 1	0.44 [0.37 0.53]	1.03e-14 [0 3.46e-09]	100
	Model 2	0.10 [0.053 0.16]	0.40 [0.022 0.96]	0
	Model 3	0.10 [0.061 0.17]	0.36 [0.016 0.92]	0
	Model 4	0.091 [0.053 0.15]	0.44 [0.038 0.96]	0
Data gap duration	Model 1	0.22 [0.11 0.30]	0.0014 [7.67e-07 0.29]	42
	Model 2	0.20 [0.12 0.28]	0.0025 [1.12e-05 0.19]	35
	Model 3	0.11 [0.078 0.16]	0.24 [0.034 0.70]	0
	Model 4	0.12 [0.072 0.18]	0.18 [0.0084 0.73]	0

Table 3
Jensen-Shannon divergence calculated for each gap characteristic in the adult population.

	Jensen-Shannon divergence		
	Median [5th-95th percentile]		
	Number of gaps per sensor	Relative day when data gap occurred	Data gap duration
Model 1	0.1714 [0.1195 0.2353]	0.2103 [0.1638 0.2680]	0.0843 [0.0566 0.1211]
Model 2	0.1731 [0.1176 0.2470]	0.0423 [0.0209 0.0760]	0.0882 [0.0545 0.1211]
Model 3	0.1641 [0.1189 0.2222]	0.0453 [0.0286 0.0659]	0.0654 [0.0325 0.1043]
Model 4	0.1141 [0.0700 0.1597]	0.0486 [0.0265 0.0742]	0.0616 [0.0368 0.0911]

agement strategies to be tested in more realistic simulation scenarios. Previous efforts to model data gaps were limited to datasets collected only in adults, using past-generation CGM sensors, which required periodic in vivo calibrations and had limited accuracy. The purpose of this work was to develop a data gap model that can describe well the main data gap characteristics for a recent factory-calibrated CGM sensor, on both the adult and the pediatric population.

Two datasets were used for this study, both collected by the Dexcom G6 sensor: the first dataset includes 172 traces collected in adults, the second 205 traces collected in pediatrics. The model was developed by attempting to match the observed distribution of three gap characteristics: the number of gaps per sensor, the relative day when data gaps occurred, and the data gap duration. In total four candidate Markov models, of increasing complexity, were proposed. Each model was identified on a training set (70% of the data) and then tested on a test set (30% of the data), using the Kolmogorov-Smirnov test and the Jensen-Shannon divergence.

The best data gap model was found to be a six-state Markov model (Model 4), in which two states describe, respectively, the normal operation of a sensor that has never had a gap and the normal operation of a sensor that has already had at least one gap, and four states describe the occurrence of missing samples. The total number of model parameters is 9 for the adult population and 11 for the pediatric population (in the adult population, 2 parameters were removed with no performance deterioration). This six-state Markov model presented satisfactory performances in both populations for all three data gap characteristics.

The current study presents some limitations. A first limitation concerns the fact that the proposed models have been developed considering only CGM traces with minimum duration of 9 days, i.e., sensors with a normal lifetime of about 10 days. In fact, modeling the premature stopping of sensor operation – a fault other than data gaps, due to potentially irreversible damage of the sensor – was outside the scope of this work. Therefore, the domain of validity of the developed data gap models must be considered limited to sensors with a lifetime of 9-10 days. Another limitation of the present work is that the modeling of CGM data gaps is performed independently of other characteristics of the CGM signal, such as the glucose concentration level, the glucose rate-of-change, other sensor error components (e.g., the distortion introduced by plasma-interstitium kinetics, the calibration error and the random noise), and other faults (e.g., compression artifacts and the premature stopping of sensor operation). Although in a preliminary analysis conducted on the adult dataset no significant correlation was found between data gap characteristics and other CGM signal characteristics (specifically, the glucose level at which data gaps begin, and the parameters of the sensor error model by Vettoretti et al. [27] – the results not shown for reasons of space), further analyses are required to investigate whether other factors have a relevant impact on the occurrence and the duration of gaps, and thus need to be considered as additional variables within the data gap model (e.g., using a different multivariable modeling approach). For example, it would be interesting to investigate whether premature stopping of sensor operation has an impact on the characteristics of the gaps observed before the end of the sensor's life, and possibly to develop a new model that jointly describes these two types of sensor faults.

Despite these limitations, the proposed six-state Markov model describes well the analyzed gap characteristics (the number of gaps per sensor, the relative day when data gaps occurred, and the data gap duration) in both the adult and the pediatric population. Nevertheless, the model description of the gap number per sensor could be further improved, trying to reduce the overestimation in the description of the number of traces that contain a single event. This could be addressed by future modeling studies. Other interesting future developments of the Markov model presented in this work could be the external validation of the model on other datasets acquired by the Dexcom G6 sensor and its application on datasets collected by other CGM sensors. Last but not least, the model identified in this work can be integrated into diabetes simulators (e.g., the T1D patient decision simulator [33]) used to test CGM-based therapies in realistic ISCTs.

5. Conclusions

In conclusion, in this paper we developed a new model of CGM data gaps that describes well the number of gaps per sensor, the monitoring days when gaps occur, and the gap durations, by exploiting two datasets collected by the Dexcom G6 sensor on an adult and a pediatric population, respectively. The final model is a six-state Markov model in which four states are used for describing gaps and the other two for describing the normal operation of the sensor. The model performance was evaluated on an independent test set. The modelling methodology presented in this paper can be extended to other CGM sensors, and also to time series collected with other types of sensors. This model is useful to study the occurrence of gaps in CGM sensors, to compare them between different sensors [45], and to realistically simulate gaps on virtual CGM traces generated by diabetes simulators. The ability to realistically simulate gaps is critical to enable the simulation of realistic CGM traces in ISCTs testing CGM-based diabetes therapies. Finally, the model can be useful to test signal reconstruction algorithms that aim to reconstruct the CGM signal suppressed during gaps [46].

Declaration of Competing Interest

The authors have no conflict of interest to declare.

Acknowledgements

The datasets used in this paper are courtesy of Dexcom Inc. (San Diego, CA).

Funding

Part of this work was supported by MUR (Italian Ministry for University and Research) under the initiative “Departments of Excellence” (Law 232/2016).

Supplementary materials

Supplementary material associated with this article can be found, in the online version, at doi:10.1016/j.cmpb.2023.107700.

References

[1] RW Beck, RM Bergenstal, LM Laffel, JC. Pickup, Advances in technology for management of type 1 diabetes, Lancet 394 (10205) (2019) 1265–1273, doi:10.1016/S0140-6736(19)31142-0.
[2] K Dovc, T. Battelino, Evolution of Diabetes Technology, Endocrinol Metab Clin North Am 49 (1) (2020) 1–18, doi:10.1016/j.ecl.2019.10.009.
[3] J. Pickup, Insulin pumps, Int J Clin Pract Suppl (170) (2011) 16–19, doi:10.1111/j.1742-1241.2010.02574.x.
[4] R Nimri, J Nir, M. Phillip, Insulin Pump Therapy, Am J Ther 27 (1) (2020) e30–e41, doi:10.1097/MJT.0000000000001097.
[5] DC Klonoff, D Ahn, A. Drincic, Continuous glucose monitoring: A review of the technology and clinical use, Diabetes Res Clin Pract 133 (2017) 178–192, doi:10.1016/j.diabres.2017.08.005.
[6] O Didyuk, N Econom, A Guardia, K Livingston, U. Klueh, Continuous Glucose Monitoring Devices: Past, Present, and Future Focus on the History and Evolution of Technological Innovation, J Diabetes Sci Technol 15 (3) (2021) 676–683 May, doi:10.1177/1932296819899394.
[7] M Vettoretti, A. Facchinetti, Combining continuous glucose monitoring and insulin pumps to automatically tune the basal insulin infusion in diabetes therapy: a review, Biomed Eng Online 18 (1) (2019) 37, doi:10.1186/s12938-019-0658-x.
[8] H Thabit, R. Hovorka, Coming of age: the artificial pancreas for type 1 diabetes, Diabetologia 59 (9) (2016) 1795–1805, doi:10.1007/s00125-016-4022-4.
[9] SJ Moon, I Jung, CY. Park, Current Advances of Artificial Pancreas Systems: A Comprehensive Review of the Clinical Evidence, Diabetes Metab J 45 (6) (2021) 813–839, doi:10.4093/dmj.2021.0177.
[10] NS Tyler, PG. Jacobs, Artificial Intelligence in Decision Support Systems for Type 1 Diabetes, Sensors (Basel) 20 (11) (2020) 3214, doi:10.3390/s20113214.
[11] M Vettoretti, G Cappon, A Facchinetti, G. Sparacino, Advanced Diabetes Management Using Artificial Intelligence and Continuous Glucose Monitoring Sensors, Sensors (Basel) 20 (14) (2020) 3870 Jul 10, doi:10.3390/s20143870.
[12] F Pappalardo, G Russo, FM Tshinanu, Viceconti M. In, silico clinical trials: concepts and early adoptions, Brief Bioinform 20 (5) (2019) 1699–1708 Sep 27, doi:10.1093/bib/bby043.
[13] M Viceconti, C Cobelli, T Haddad, A Himes, B Kovatchev, M. Palmer, In silico assessment of biomedical products: The conundrum of rare but not so rare events in two case studies, Proc Inst Mech Eng H 231 (5) (2017) 455–466 May, doi:10.1177/0954411917702931.
[14] A. Facchinetti, Continuous Glucose Monitoring Sensors: Past, Present and Future Algorithmic Challenges, Sensors (Basel) 16 (12) (2016) 2093, doi:10.3390/s16122093.
[15] C Cobelli, C Dalla Man, Minimal and Maximal Models to Quantitate Glucose Metabolism: Tools to Measure, to Simulate and to Run in Silico Clinical Trials, J Diabetes Sci Technol 16 (5) (2022) 1270–1298, doi:10.1177/19322968211015268.
[16] K Fritzen, L Heinemann, O. Schnell, Modeling of Diabetes and Its Clinical Impact, J Diabetes Sci Technol 12 (5) (2018) 976–984, doi:10.1177/1932296818785642.
[17] C Roversi, M Vettoretti, S Del Favero, A Facchinetti, P Choudhary, G. Sparacino, Impact of Carbohydrate Counting Error on Glycemic Control in Open-Loop Management of Type 1 Diabetes: Quantitative Assessment Through an In Silico Trial, J Diabetes Sci Technol 16 (6) (2022) 1541–1549 Nov, doi:10.1177/19322968211012392.
[18] JK Kirk, J. Stegner, Self-monitoring of blood glucose: practical aspects, J Diabetes Sci Technol 4 (2) (2010) 435–439 Mar 1, doi:10.1177/193229681000400225.
[19] C Chen, XL Zhao, ZH Li, ZG Zhu, SH Qian, AJ. Flewitt, Current and Emerging Technology for Continuous Glucose Monitoring, Sensors (Basel) 17 (1) (2017) 182 Jan, doi:10.3390/s17010182.
[20] M Vettoretti, G Cappon, G Acciaroli, A Facchinetti, G. Sparacino, Continuous Glucose Monitoring: Current Use in Diabetes Management and Possible Future Applications, J Diabetes Sci Technol 12 (5) (2018) 1064–1071 Sep, doi:10.1177/1932296818774078.
[21] J Kravarusic, G. Aleppo, Diabetes Technology Use in Adults with Type 1 and Type 2 Diabetes, Endocrinol Metab Clin North Am 49 (1) (2020) 37–55 Mar, doi:10.1016/j.ecl.2019.10.006.
[22] G Cappon, G Acciaroli, M Vettoretti, A Facchinetti, G. Sparacino, Wearable Continuous Glucose Monitoring Sensors: A Revolution in Diabetes Treatment, Electronics. 6 (3) (2017) 65 Sept, doi:10.3390/electronics6030065.
[23] G Cappon, M Vettoretti, G Sparacino, A. Facchinetti, Continuous Glucose Monitoring Sensors for Diabetes Management: A Review of Technologies and Applications, Diabetes Metab J 43 (4) (2019) 383–397 Aug, doi:10.4093/dmj.2019.0121.
[24] G Freckmann, S Pleus, M Grady, S Setford, B. Levy, Measures of Accuracy for Continuous Glucose Monitoring and Blood Glucose Monitoring Devices, J Diabetes Sci Technol 13 (3) (2019) 575–583 May, doi:10.1177/1932296818812062.
[25] F Boscari, M Vettoretti, F Cavallin, AML Amato, A Uliana, V Vallone, A Avogaro, A Facchinetti, D. Bruttomesso, Implantable and transcutaneous continuous glucose monitoring system: a randomized cross over trial comparing accuracy, efficacy and acceptance, J Endocrinol Invest 45 (1) (2022) 115–124 Jan, doi:10.1007/s40618-021-01624-2.
[26] RP Wadwa, LM Laffel, VN Shah, SK. Garg, Accuracy of a Factory-Calibrated, Real-Time Continuous Glucose Monitoring System During 10 Days of Use in Youth and Adults with Diabetes, Diabetes Technol Ther 20 (6) (2018) 395–402 Jun, doi:10.1089/dia.2018.0150.
[27] M Vettoretti, C Battocchio, G Sparacino, A. Facchinetti, Development of an Error Model for a Factory-Calibrated Continuous Glucose Monitoring Sensor with 10-Day Lifetime, Sensors (Basel) 19 (23) (2019) 5320 Dec 3, doi:10.3390/s19235320.
[28] A Facchinetti, S Del Favero, G Sparacino, JR Castle, WK Ward, C. Cobelli, Modeling the glucose sensor error, IEEE Trans Biomed Eng 61 (3) (2014) 620–629 Mar, doi:10.1109/TBME.2013.2284023.

[29] M Schiavon, G Acciaroli, M Vettoretti, A Giaretta, R. Visentin, A Model of Acetaminophen Pharmacokinetics and its Effect on Continuous Glucose Monitoring Sensor Measurements, Annu Int Conf IEEE Eng Med Biol Soc 2018 (2018) 159–162 Jul, doi:10.1109/EMBC.2018.8512257.
[30] A Facchinetti, S Del Favero, G Sparacino, C. Cobelli, Modeling Transient Disconnections and Compression Artifacts of Continuous Glucose Sensors, Diabetes Technol Ther 18 (4) (2016) 264–272 Apr, doi:10.1089/dia.2015.0250.
[31] CD Man, F Micheletto, D Lv, M Breton, B Kovatchev, C. Cobelli, The UVA/PADOVA Type 1 Diabetes Simulator: New Features, J Diabetes Sci Technol 8 (1) (2014) 26–34 Jan, doi:10.1177/1932296813514502.
[32] R Visentin, E Campos-Náñez, M Schiavon, D Lv, M Vettoretti, M Breton, BP Kovatchev, C Dalla Man, C Cobelli, The UVA/Padova Type 1 Diabetes Simulator Goes From Single Meal to Single Day, J Diabetes Sci Technol 12 (2) (2018) 273–281 Mar, doi:10.1177/1932296818757747.
[33] M Vettoretti, A Facchinetti, G Sparacino, C Cobelli, Type-1 Diabetes Patient Decision Simulator for In Silico Testing Safety and Effectiveness of Insulin Treatments, IEEE Trans Biomed Eng 65 (6) (2018) 1281–1290 Jun, doi:10.1109/TBME.2017.2746340.
[34] N Camerlingo, M Vettoretti, S Del Favero, G Cappon, G Sparacino, A Facchinetti, A Real-Time Continuous Glucose Monitoring-Based Algorithm to Trigger Hypotreatments to Prevent/Mitigate Hypoglycemic Events, Diabetes Technol Ther 21 (11) (2019) 644–655, doi:10.1089/dia.2019.0139.
[35] GJ Smith, MB Abraham, M de Bock, et al., Impact of Missing Data on the Accuracy of Glucose Metrics from Continuous Glucose Monitoring Assessed Over a 2-Week Period, Diabetes Technol Ther 25 (5) (2023) 356–362, doi:10.1089/dia.2022.0101.
[36] M Breton, B. Kovatchev, Analysis, modeling, and simulation of the accuracy of continuous glucose sensors, J Diabetes Sci Technol 2 (5) (2008) 853–862 Sep, doi:10.1177/193229680800200517.
[37] DJ Lunn, C Wei, R Hovorka, Fitting dynamic models with forcing functions: application to continuous glucose monitoring in insulin therapy, Stat Med 30 (18) (2011) 2234–2250 Aug 15, doi:10.1002/sim.4254.
[38] A Facchinetti, S Del Favero, G Sparacino, C. Cobelli, Model of glucose sensor error components: identification and assessment for new Dexcom G4 generation devices, Med Biol Eng Comput 53 (12) (2015) 1259–1269 Dec, doi:10.1007/s11517-014-1226-y.
[39] L Biagi, CM Ramkissoon, A Facchinetti, Y Leal, J. Vehi, Modeling the Error of the Medtronic Paradigm Veo Enlite Glucose Sensor, Sensors (Basel) 17 (6) (2017) 1361 Jun 12, doi:10.3390/s17061361.
[40] M Drecogna, M Vettoretti, SD Favero, A Facchinetti, G. Sparacino, Data Gap Modeling in Continuous Glucose Monitoring Sensor Data, Annu Int Conf IEEE Eng Med Biol Soc 2021 (2021) 4379–4382, doi:10.1109/EMBC46164.2021.9629588.
[41] RP Wadwa, LM Laffel, VN Shah, SK. Garg, Accuracy of a Factory-Calibrated, Real-Time Continuous Glucose Monitoring System During 10 Days of Use in Youth and Adults with Diabetes, Diabetes Technol Ther 20 (6) (2018) 395–402, doi:10.1089/dia.2018.0150.
[42] VN Shah, LM Laffel, RP Wadwa, SK. Garg, Performance of a Factory-Calibrated Real-Time Continuous Glucose Monitoring System Utilizing an Automated Sensor Applicator, Diabetes Technol Ther 20 (6) (2018) 428–433, doi:10.1089/dia.2018.0143.
[43] TB Arnold, JW. Emerson, Nonparametric Goodness-of-Fit Tests for Discrete Null Distributions, The R Journal 3 (2) (2011) 34–39 Dec, doi:10.32614/rj-2011-016.
[44] F. Nielsen, On the Jensen-Shannon Symmetrization of Distances Relying on Abstract Means, Entropy (Basel) 21 (5) (2019) 485 May 11, doi:10.3390/e21050485.
[45] F Boscari, M Vettoretti, AML Amato, V Vallone, A Uliana, E Iori, A Avogaro, A Facchinetti, D. Bruttomesso, Comparing the accuracy of transcutaneous sensor and 90-day implantable glucose sensor, Nutr Metab Cardiovasc Dis 31 (2) (2021) 650–657 Feb 8, doi:10.1016/j.numecd.2020.09.006.
[46] SJ Fonda, DG Lewis, RA. Vigersky, Minding the gaps in continuous glucose monitoring: a method to repair gaps to achieve more accurate glucometrics, J Diabetes Sci Technol 7 (1) (2013) 88–92 Jan 1, doi:10.1177/193229681300700110.